

# Geomorphic limits to climate-induced increases in topographic relief

Kelin X Whipple, Eric Kirby & Simon H. Brocklehurst

Department of Earth, Atmospheric and Planetary Sciences, Massachusetts Institute of Technology, Cambridge, Massachusetts 02139, USA

**Recognition of the potential for strong dynamic coupling between atmospheric and tectonic processes has sparked intense cross-disciplinary investigation and debate on the question of whether tectonics have driven long-term climate change or vice versa. It has been proposed that climate change might have driven the uplift of mountain summits through an isostatic response to valley incision. Because isostasy acts to compensate mean elevations, the debate hinges on the question of whether climate change can significantly increase topographic relief or, more precisely, increase the volume of ‘missing mass’ between summits and ridges. Here we show that, in tectonically active mountain ranges, geomorphic constraints allow only a relatively small increase in topographic relief in response to climate change. Thus, although climate change may cause significant increases in denudation rates, potentially establishing an important feedback between surficial and crustal processes, neither fluvial nor glacial erosion is likely to induce significant isostatic peak uplift.**

There is increasing recognition that geodynamic and geothermal responses to surface erosion and relief production provide a direct linkage between climate-driven denudation and tectonic processes<sup>1,2</sup>. The coupled effects of topographic relief evolution and erosional unloading importantly influence the following: (1) isostatically compensated mountain summit elevations<sup>3,4</sup> and thus interpretation of landscape morphology in terms of tectonic surface uplift<sup>5,6</sup>; (2) spatial and temporal partitioning of tectonic and isostatic rock uplift, with potential direct feedback loops between zones of focused denudation and relief production and zones of focused crustal strain<sup>1,2</sup>; and (3) near-surface geothermal gradients and thus interpretation of thermochronological data in terms of rock exhumation rates<sup>7,8</sup>. The evolution of relief in response to climate change in particular is important in the debate over potential linkages between late Cenozoic uplift of the Himalayas and the Tibetan plateau and the onset of Quaternary glaciation<sup>3,5,9</sup>.

Molnar and England<sup>5</sup> argued that evidence cited for accelerated rates of Quaternary tectonism might in fact be produced by enhanced rates of valley incision induced by Quaternary climate change to stormier and/or glaciated conditions. The crux of the argument and central to the ensuing debate is the hypothesis that Quaternary climate change not only accelerated erosion but also caused a significant increase in topographic relief<sup>3,6,10,11</sup>. Although some supporting data have been obtained<sup>6,10</sup>, no convincing empiri-

cal evidence for significant climate-induced Quaternary peak uplift has been produced. Moreover, no comprehensive analysis of quantitative limitations to relief production in either glacial or non-glacial environments has hitherto been presented.

Here we provide a quantitative overview of the processes of erosion and relief production. We specifically focus on the question of the amount of relief production (or reduction) that can be expected from a change to a more erosive climate. We consider in turn the effects of an increase in fluvial erosivity, and the effects of a transition from fluvial to glacial erosion. Where current understanding of the erosion processes is insufficient to provide quantitative constraints (for example, glacial erosion), we cite empirical evidence and attempt to outline critical outstanding problems. We limit our focus to tectonically active orogens, intentionally avoiding the well known, limiting case of climate-induced incision into an undissected, elevated plateau<sup>4,5</sup>.

## Scales of relief

As with most morphometric parameters, relief varies with the scale of measurement, generally increasing with scale up to approximately the half-width of the mountain range. Thus it is necessary first to define measures of relief pertinent to the problem of isostatic response to denudation. Although relief varies over a continuum of scales, it is useful to define three fundamental components of relief: hillslope relief, tributary channel relief (elevation drop along tributaries), and trunk channel relief (elevation drop along the trunk channel) (Fig. 1). The sum of hillslope relief and trunk channel relief is equivalent to the often-used “drainage basin relief”. Similarly, the sum of hillslope relief and tributary channel relief is roughly analogous to the commonly used measure of ridge line to valley bottom relief<sup>3,4,12,13</sup>. In the case of non-glacial landscapes, channel relief must be further subdivided into colluvial, bedrock, and alluvial channel components (Fig. 1), owing to differences in operative erosion processes in each<sup>14</sup>. Colluvial channels are those channels where erosion is dominantly by debris-flow scour<sup>15,16</sup>. In the case of glaciated landscapes, channel relief is simply the elevation drop on glaciated valley floors plus the elevation drop on bedrock and alluvial channels below the glacial limit.

## Relief production in fluvial landscapes

Hillslope relief in tectonically active orogens is dictated by drainage density, and therefore hillslope lengths<sup>17</sup>, and rock mass strength<sup>18,19</sup>. Here “tectonically active” can be defined as a condition in which rates of rock uplift, and commensurate channel incision, are greater

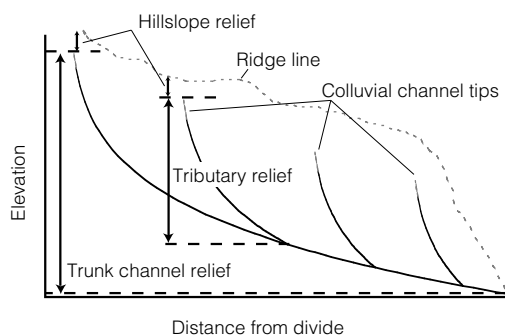


**Figure 1** Sketch showing definitions of the components of fluvial relief. Heavy solid lines show trunk and tributary channel profiles projected onto a vertical plane through the axis of the drainage basin. Grey solid lines show debris-flow dominated or ‘colluvial’ channel tips. The light dashed line is a schematic representation of ridge line elevations projected onto the same plane as the channel profiles. Heavy dashed lines are horizontal reference lines used to define the various (labelled) components of relief. Downstream alluvial channel reaches are not shown.

than soil production rates<sup>20</sup> such that slopes are stripped of soil, and hillslope denudation is dominated by deep-seated landsliding<sup>19,21,22</sup>. Under these conditions, frequency distributions of hillslope gradients rapidly attain a maximum or saturation state beyond which they are statistically invariant<sup>19</sup> (Table 1). With the exception of brief transients in which hillslopes may be temporarily oversteepened by rapid incision, hillslope relief in active orogens can only be increased by a decrease in drainage density. However, Schmidt and Montgomery<sup>18</sup> have shown that longer hillslopes are less stable, and therefore hillslope relief itself probably reaches a maximum. Thus, a change of climate to a more erosive fluvial environment cannot significantly increase the hillslope component of relief in a tectonically active orogen<sup>3</sup>. Indeed, increasing the erosivity of the fluvial system is likely to increase drainage density, producing a commensurate decrease in hillslope relief<sup>23</sup>.

Relief evolution in fluvial environments is most strongly dependent on the response of the bedrock channel system. Alluvial channels have gentle gradients, typically occur only in the foreland and foothills of active mountain ranges, and thus contribute little to overall relief. In addition, although the controls on the extent of colluvial channels are not well known, evidence from tectonically active non-glacial mountain ranges suggests that the elevation drop on bedrock channels typically comprises 80–90% of drainage basin relief (Fig. 1; Table 2). Therefore, with the caveat that the dynamics and extent of colluvial channels are at present poorly known<sup>24</sup>, an analysis of the response of bedrock channel relief should represent the first-order characteristics of the evolution of relief in an unglaciated landscape.

Although many important questions remain unanswered in the study of bedrock channel erosion<sup>25,26</sup>, the well-known “stream power erosion law” appears sufficiently robust to characterize the response of the bedrock channel to a change in the erosivity of the fluvial system. According to the stream power erosion law, local erosion rate is a power-law function of upstream drainage area (that is,  $A = k_a x^h$  where  $k_a$  is a dimensional constant,  $x$  is distance downstream, and  $h$  is the reciprocal of the Hack exponent<sup>27</sup>) and channel gradient ( $S = -dz/dx$ ), such that a river profile evolution equation can be written as<sup>28</sup>:

$$\frac{dz}{dt} = U(x, t) - Kk_a^m x^{hm} \left| \frac{dz}{dx} \right|^n \quad (1)$$

where  $dz/dt$  is the rate of change of bed elevation,  $U$  is rock uplift rate (defined relative to base-level),  $K$  is a dimensional coefficient of erosion, and  $m$  and  $n$  are positive constants that reflect erosion processes, basin hydrology, and channel hydraulic geometry<sup>26,28</sup>.

The coefficient of erosion  $K$  is influenced by many climate-related factors including precipitation, storminess, sediment flux, and channel width<sup>26</sup>. The quantitative relationship between  $K$  and climate variables is complex, as these factors may adjust differently in response to a given climate change. We do not address this unresolved problem. Rather we ask the simpler question: what is the effect of a hypothetical shift to a ‘more-erosive’ (higher- $K$ ) condition? Further, we first treat the simplified case of a uniform change in  $K$  and then briefly consider the potential effects of non-uniform changes in erosivity.

Under steady-state conditions (for uniform  $K$  and  $U$ ) where erosion balances rock uplift ( $dz/dt = 0$ ), equilibrium channel gradient is a power function of drainage area ( $A$ ):

$$S = k_s A^{-\theta} \quad (2a)$$

$$k_s = (U/K)^{\frac{1}{n}}; \quad \theta = m/n \quad (2b)$$

where  $k_s$  and  $\theta$  can be termed the steepness and concavity indices, respectively. Equation (2a) is often applied in analysis of channel profile data<sup>14,29–32</sup>. Typical values of the concavity index ( $\theta$ ) for arguably equilibrium channel profiles in tectonically active fluvial landscapes given in Table 2 are consistent with theoretical predic-

**Table 1 Hillslope gradient distributions in mountainous areas**

Location	Mean slope (°)*	1σ	Source
Altunshan, China	28.7	10.6	This work†
Altuntagh, China	2.8	9.3	This work†
Tien Shan, China	32	13.8	This work†
Mekong River, Yunnan Province, China	30.5	10.9	This work†
Nanga Parbat region, Pakistan	32	~10	Ref. 19
Dan Gabriel Mtns, California, USA	3.15	8.5	This work‡
Eastern White Mtns, California, USA	34	8.2	This work‡
Western White Mtns, California, USA	34	9.2	This work‡
King Range, California, USA	33	8.3	This work‡

\* All measured slopes are averaged across 3 pixels and therefore represent minimum estimates.

† 90-m resolution digital elevation model (DEM) data (slopes strongly underestimated).

‡ 30-m resolution DEM data.

tions that the  $m/n$  ratio should fall in a narrow range near 0.5 ( $0.35 \leq m/n \leq 0.6$ ) for fluvial erosion processes<sup>26</sup>. Empirical values of  $\theta$  outside the expected range<sup>14</sup> probably reflect some combination of disequilibrium conditions, systematic downstream variation in  $K$  or  $U$ , or regression of data that cross the bedrock-alluvial transition. Under steady-state conditions and spatially invariant  $K$  and  $U$ , equation (1) can be integrated to find the equilibrium channel relief ( $R_f$ ) of a bedrock river:

$$R_f = z(x_c) - z(L) = \left(\frac{U}{K}\right)^{\frac{1}{n}} k_a^{-\frac{m}{n}} \left(1 - \frac{hm}{n}\right)^{-1} \left(L^{1-\frac{hm}{n}} - x_c^{1-\frac{hm}{n}}\right); \quad (3a)$$

$$\frac{hm}{n} \neq 1$$

$$R_f = z(x_c) - z(L) = \left(\frac{U}{K}\right)^{\frac{1}{n}} k_a^{-\frac{m}{n}} (\ln L - \ln x_c); \quad \frac{hm}{n} = 1 \quad (3b)$$

where  $L$  is the length of the bedrock stream measured from the divide, and  $x_c$  is the length of the hillslope plus any colluvial channel segment, also measured from the divide ( $x_c \approx A_c^{1/2}$ ; see Table 2). Thus equation (3) gives the elevation drop on the bedrock channel only ( $R_f$ ). We note that equation (3) shows that equilibrium bedrock channel relief varies inversely with  $K$ . Thus, for the case of a spatially constant increase in  $K$ , both tributary and trunk channel relief ultimately will be reduced in response to a shift to a more erosive climate (Fig. 2). This simple conclusion directly contradicts the commonly cited notion that increased precipitation (and presumably greater erosivity) causes greater relief along tectonically

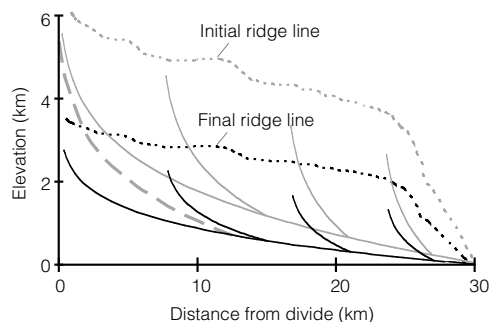


**Figure 2** Equilibrium relief in fluvial landscapes. Solid grey lines show initial steady-state trunk and tributary channel profiles in a climate with low erosive potential (that is, low  $K$  in equation (1)). Dashed grey line shows the corresponding initial ridge-line topographic envelope. Solid black lines show final steady-state trunk and tributary channel profiles in a more erosive climate (high  $K$ ). Dashed black line shows the corresponding final ridge-line topographic envelope. We have assumed that hillslope relief had already attained a maximum in the less erosive climate (rock uplift rate  $\geq$  soil production rate<sup>20</sup>). Comparison of these two steady-state conditions illustrates that a change to a more erosive climate must ultimately reduce relief in a fluvial landscape. Heavy long-dashed grey line illustrates the steepening of upper channel reaches (shown for trunk stream only) required to induce an increase in relief.

**Table 2 Relief statistics in tectonically active fluvial landscapes**

Field area	Crit. drainage area* $A_c$ ( $10^3$ m <sup>2</sup> )	Avg. colluvial slope, $S_c$ (m/m)	Fluvial relief, $R_f/R_t$ (%)	Concavity index†, $\theta$	No of drainages, $N$
King Range, California, USA (high uplift rate)	$0.59 \pm 0.20$	$0.54 \pm 0.11$	$79 \pm 7$	$0.40 \pm 0.10$	14
King Range, California, USA (low uplift rate)	$0.72 \pm 0.24$	$0.36 \pm 0.05$	$80 \pm 5$	$0.49 \pm 0.10$	7
Central Range, Taiwan	$1.40 \pm 0.48$	$0.63 \pm 0.26$	$89 \pm 6$	$0.41 \pm 0.1$	4

All uncertainties indicate  $1\sigma$ -error bars.

\* Defined by the break in slope–area scaling in longitudinal profile data.

† Defined by equation (2) in the text; reported values are fits to long profile data between  $A_c$  and the bedrock–alluvial transition only.

active mountain fronts<sup>12,13</sup>. Despite the reduction in relief, the transition to a more erosive condition does increase rates of channel incision, and therefore rates of hillslope denudation by landsliding. However, the enhanced erosion is concentrated in the upper part of drainage basins as channels cut down to lower equilibrium gradients (Fig. 2). Simple geometry dictates that only a response to climate change that involves steepening of the upper reaches of the channel system in concert with accelerated incision of the trunk stream would in fact produce relief, as illustrated in Fig. 2.

Although the relief structure of landscapes is demonstrably altered during a transient response to a change in fluvial erosivity (Fig. 3), and also by non-uniform changes in  $K$  that may result from climate change<sup>14</sup>, we find that under most circumstances the steepening of headwater tributaries required to increase relief will not occur. Consider the transient response to a sudden, uniform change in  $K$ . Figure 3 shows that reduction of channel gradients first occurs along trunk streams and only later along tributary and headwater stream segments, resulting in a transient increase in channel concavity. However, as nowhere in the system are channel gradients increased, there is no accompanying increase in relief. Rather, the transient response is characterized by an upstream propagating wave of relief reduction (Fig. 3).

Spatially non-uniform increases in  $K$  generally produce similar effects. As long as  $K$  is everywhere increased, all channel gradients and therefore relief (both transient and steady state) will be reduced. If a given climate change causes  $K$  to be preferentially increased in downstream channel segments, transients will be shorter-lived and final steady-state channel profiles will resemble the transient profiles shown in Fig. 3, and relief will be similarly diminished. Conversely, if  $K$  is preferentially increased in upstream channel segments both channel gradient and concavity will be reduced, resulting in a greater relief reduction than in the uniform- $K$  case. Thus, only a climate change which induces a decrease in  $K$  along headwater channel segments in concert with an increase in  $K$  downstream can be expected to increase relief. Although one may imagine a few

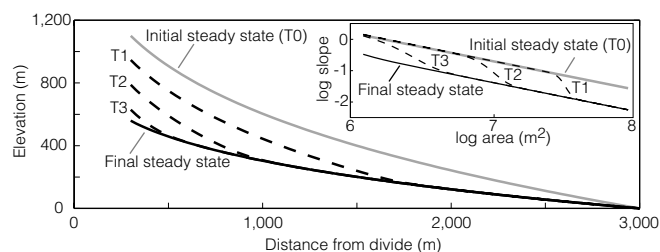


**Figure 3** Numerical simulation of the transient response of a channel profile to a sudden, uniform increase in erosivity. (Shown is the effect of a two-fold increase in  $K$  in equation (1).) Inset shows the transient response in slope–area space (log–log scale). Both the main panel and inset shows the initial steady-state profile (T0; solid grey), three intermediate transient profiles, sequentially T1, T2, and T3 (black dashed lines), and the final steady-state profile (solid black). The transient response is characterized by an upstream-propagating wave of gradient, and therefore relief, reduction. Nowhere in the system are channel gradients increased (see inset). Note that if  $K$  were unchanged over the first kilometre of channel length and doubled only downstream of this point, the final steady-state solution would approximately coincide with the T2 transient profile.

scenarios in which this could occur (for example, enhanced fluvial discharge but reduced frequency of debris flows in headwater colluvial channels), we are unaware of any evidence that such changes are representative of Quaternary climate change or that the resulting increase in relief would be significant. Further study of such non-uniform changes in erosivity is warranted.

**Relief production in glaciated landscapes**

The isolated spires, narrow ridges, long bare-rock hillslopes, and broad valleys of alpine terrain immediately give a qualitative impression that glaciers are highly efficient erosive agents and that glacial erosion produces considerable relief. This sense of the production of relief, now supported by data showing that erosion by fast-moving temperate glaciers can far outpace that expected for rivers<sup>33</sup>, led Molnar and England<sup>5</sup> to suggest that a transition to glacial erosion could induce significant isostatic peak uplift. However, such an effect has not been demonstrated empirically<sup>6</sup>, and even the premise that glacial erosion produces a net increase in relief has been challenged<sup>11</sup>.

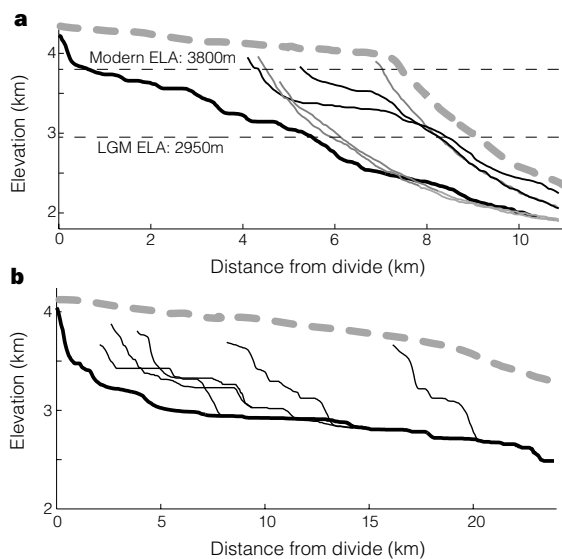


**Figure 4** Relief structure of glaciated landscapes. **a**, Comparison of adjacent unglaciated (solid grey lines), partially glaciated (solid black lines), and fully glaciated (heavy black line) drainage basins along the eastern flank of the Sierra Nevada, near Lone Pine, California. Heavy dashed grey line illustrates the topographic envelope of ridges and peaks. Horizontal dashed lines indicate the modern and late Pleistocene positions of the equilibrium line altitude (ELA) in this part of the Sierra Nevada. Glacial valley lowering has been most effective at elevations between the modern and late Pleistocene ELAs, resulting in reduced valley profile concavity in the glaciated zone and a commensurate reduction of valley profile relief. Although there are some indications of ridge-to-valley relief increases at the mid-basin position, hillslope relief increases do not appear to have fully compensated for the reduction of valley profile relief. **b**, Relief structure of the Dinwoody Creek basin, northwestern Wind River Range, Wyoming, showing trunk valley profile (heavy black line), tributary profiles (black lines), and the topographic envelope of a pre-glacial low-relief surface<sup>6</sup> (heavy dashed grey line). Hillslope relief on the trunk and tributary profiles averages ~400 m. Hanging valley relief ranges from 200 to 400 m.

As the mechanics of glacial erosion are less well known (there is no equivalent of a stream power erosion law for glaciers), our analysis of glaciated landscapes is perforce more qualitative and preliminary than the above argument for fluvial landscapes. Here we outline the characteristics of glacial erosion which are likely to alter the relief structure of a pre-existing fluvial landscape in an attempt to (1) place general constraints on the likely magnitude of relief production during a transition to glaciated conditions and (2) identify critical outstanding problems. We first consider relief-production and then relief-reduction mechanisms. Our analysis considers only temperate glaciers with wet bases, ignoring for the moment some potentially important effects of the possible occurrence of basal freezing along the upper reaches of thin, high-altitude alpine glaciers<sup>34,35</sup>.

From study of alpine landforms (Fig. 4) in a range of geological and tectonic environments, and from consideration of the mechanics of alpine glacial erosion, we reason that glacial erosion may produce relief through four main mechanisms: valley widening, ice buttressing of rock slopes, and formation of hanging valleys and overdeepenings. Widening of V-shaped fluvial valleys is a natural consequence of erosion by thick masses of slowly moving ice<sup>36</sup>. Narrow ridges between first-order side tributaries are erased as tributaries are replaced by hillslopes (Fig. 5a) and wide ridges between the main tributaries are reduced to narrow knife-edged ridges and spurs. The net effect is a decrease in drainage density with a commensurate lengthening of hillslopes, thus increasing the 'missing mass' in valleys. In addition, hillslope relief can be further increased during glacial incision (Fig. 5a) because of the stabilizing effect of buttressing by thick ice masses, despite long-term constraints on hillslope relief due to landsliding<sup>18,19</sup>. Although landslides following glacial retreat are common, the long, oversteepened

bare-rock slopes of many formerly glaciated valleys (Fig. 4) indicate that this transient increase in hillslope relief is long lived compared to isostatic response times. The formation of hanging valleys effectively insulates ridge line lowering from lowering in the main valley (Fig. 5b), thus increasing tributary or 'valley' relief. However, the additional 'missing mass' associated with hanging-valley relief is limited to material removed along the axis of the trunk valley itself. Finally, glaciers are able to erode below fluvial base-level, as reflected in the formation of overdeepenings such as fjords, which adds an additional component of relief production.

Acting in direct opposition to these relief-production mechanisms, we identify three mechanisms by which glacial erosion may cause a reduction in some components of relief: concentration of erosion at higher elevations<sup>11</sup>, reduction of fluvial erosion downstream of glaciers, and possible acceleration of summit-lowering rates in the near-glacial environment. Accelerated glacial erosion and the associated relief-generation mechanisms listed above naturally only occur above the ice limit, with most erosion focused around the position of the equilibrium line altitude (ELA), where ice flux reaches a maximum<sup>37</sup>. As with climate-induced increases in fluvial erosion, glacial erosion is therefore concentrated in the upper parts of drainage basins and must contribute to a reduction of the elevation fall along the trunk valley profile (Fig. 5c). This effect is clearly shown in the longitudinal profiles of glacial valleys carved by wet-based temperate glaciers. Glacial valley profiles are not only significantly less steep but also less concave than fluvial bedrock channel profiles (Fig. 4a). Analyses of glaciated valley profiles in the western US reveal consistently lower concavity than typical fluvial valleys ( $\theta = 0.18 \pm 0.08(1\sigma)$ , determined for 16 glaciated drainages in the Sierra Nevada, Wind River, Bitterroot, and Wasatch Ranges, compared with 0.35–0.6 for bedrock fluvial channels). Also, aggradation caused by large increases in sediment flux associated with glacial erosion<sup>33</sup> will bury bedrock channels in alluvium; this will reduce rates of bedrock channel lowering below the glacial limit<sup>14,24</sup>, thereby acting to further limit relief production along the trunk stream (Fig. 5c). Finally, periglacial processes may accelerate the rate of summit erosion and thus diminish any potential relief increases, although no data have as yet demonstrated this effect<sup>6</sup>.

Whether glacial erosion deepens valleys, and thus induces an isostatic uplift of peaks and ridges<sup>5,6</sup>, or acts to plane off mountain ranges at (or somewhat above) the ELA<sup>11</sup> depends on the relative efficacy of the above relief-generation and relief-reduction mechanisms. Unfortunately, the mechanics of glacial erosion and relief production are insufficiently well known at present to permit definitive, quantitative answers to this question. But our preliminary observations in a wide range of glaciated landscapes lead us to suggest that relief increases attributable to most of the above-cited mechanisms scale with ice thickness, and therefore produce only limited additional relief. For instance, the potential increase of relief due to the ice buttressing effect and the width of parabolic glacial valley cross-sections both depend directly on ice thickness. Similarly, as the surfaces of tributary ice streams typically meet at the same elevation (that is, tributary ice falls are rare during full-glacial times), hanging valley relief must scale with the difference in ice thickness. If this ice-thickness hypothesis stands the test of time, and if no other as yet unrecognized relief-production mechanisms come to light, the implication is that average basin-wide relief production by wet-based temperate glaciers may be limited to several hundred metres (of the order of typical ice thicknesses).

Although the formation of hanging valleys and overdeepenings may entail the production of considerable amounts of vertical relief (with as many as 2–4 hanging valley or overdeepening steps between ridge lines and trunk stream valley bottoms in large basins), only a small percentage of the land surface areas is affected by this incision because most of the land surface is insulated behind hanging valley steps. The study by Small and Anderson<sup>6</sup> of Quaternary relief production by glacial erosion in the Wind River Range, Wyoming,

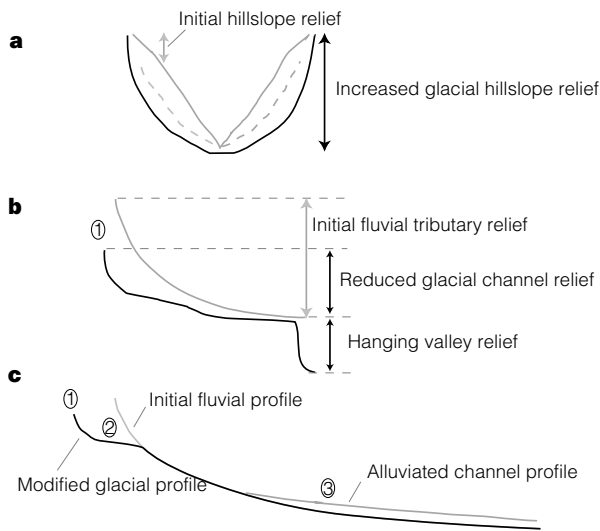


**Figure 5** Glacial relief adjustment mechanisms. **a**, An initial V-shaped valley defined by ridge lines (solid grey) and channel profiles (dashed grey) of steep first-order tributaries, and a modified U-shaped glacial valley profile (solid black). Glacial valley widening and ice-buttressing of hillslopes together result in the obliteration of small tributary valleys, reduction in drainage density, and an increase in hillslope relief (indicated). **b**, An initial fluvial tributary channel profile and relief (grey lines) and modified glacial tributary valley and hanging valley profiles and relief (black lines). The formation of hanging valleys adds an important component of relief in glaciated landscapes, effectively insulating ridge lines from trunk valley incision. However, reductions in both slope and concavity of glacial valley profiles tends to reduce relief along tributary valley profiles. The net change in relief depends critically on the relative magnitude of hillslope relief increases above the tributary valleys (at location 1). **c**, Relief adjustments along longitudinal profiles of glaciated valleys are affected by: hillslope relief increases in the glaciated zone (location 1), reduced concavity and slope of valley profile in the glaciated zone (location 2), and alluviation of downstream fluvial bedrock channel reaches (location 3), which acts to further inhibit relief production.



serves as an excellent example of this effect.

Small and Anderson<sup>6</sup> document glacial valley deepening of ~800 m into a pre-existing high-elevation but low-relief surface. Figure 4b shows the relief structure of a typical glacial valley in the Wind River Range. Most of the valley deepening is clearly accounted for by enhanced hillslope relief (~400 m) and the drop on hanging valleys (200–400 m). Despite the great depth of the trunk glacial valleys, however, the formation of hanging valleys restricts the total volume of mass removal associated with this incision. Accordingly, by dividing their estimate of the total volume of ‘missing mass’ by land surface area, Small and Anderson<sup>6</sup> compute an average Quaternary relief production of the order of 300 m. The Late Pleistocene glaciers that carved these valleys were relatively thick, of the order of 300–400 m, as indicated by erosional trimlines and estimations based on valley slope<sup>34</sup>; this is consistent with the observed hillslope and hanging valley relief and the hypothesis put forward above. Moreover, for the specific case of the Wind River Range, Small and Anderson conclude that there has been negligible isostatic uplift of summit surfaces during the Quaternary—despite the nearly 300 m of relief production—due to the action of slow but non-negligible (~0.01 mm yr<sup>-1</sup>) summit lowering<sup>38</sup> and flexural distribution of the isostatic response to the erosional unloading.

### Anticipated effect of climate change on topographic relief

In tectonically active mountain belts, the increase in relief due to accelerated erosion induced by climate change, and therefore the commensurate flexural-isostatic uplift of peaks and ridges, is likely to be minimal. Indeed, in almost all non-glacial landscapes an increase in the erosivity of the fluvial system is anticipated to lead to a reduction in both trunk stream and tributary relief. When coupled with the constraint that hillslope relief rapidly attains a maximal condition in active orogens, this observation implies that ridge to valley bottom relief will actually decrease under these conditions. We note that relief increase is possible if (and only if) a given climate change induces a decrease in erosivity along headwater channel segments in concert with a simultaneous increase in erosivity farther downstream. Aspects of relief evolution in non-glacial environments that merit further study are: (1) possible increases in the relief on poorly understood colluvial, debris-flow channel segments<sup>24</sup>, (2) the magnitude and duration of possible relief increases due to transient increases in channel concavity associated with non-uniform changes in the coefficient of erosion,  $K$ , and (3) the quantitative relationship between climate variables and  $K$ .

The onset of glacial erosion is likely to involve competing effects of relief production over short wavelengths (increases in hillslope relief, valley widening, and formation of hanging valleys and overdeepenings) and relief reduction over long wavelengths (reduction of relief on trunk and tributary valley profiles). Further study is needed to quantify fully the net effects of the various relief generation and reduction mechanisms outlined here. In particular, the upper limit on transient glacial hillslope relief increases is an important unknown. In addition, if the upper reaches of thin, high-altitude alpine glaciers become frozen to their beds, ridges and peaks may be protected from erosion and glacial valley long profiles may become more concave<sup>35</sup>, adding a potentially important component to overall glacial relief production. But for the case of wet-based temperate glaciers, we argue that relief generation associated with each of the various glacial relief production mechanisms scales with ice thickness. Although the formation of a cascade of hanging valleys may entail the production of considerable amounts of vertical relief, the added ‘missing mass’ attributable to this incision is restricted by the limited areal extent of the trunk valleys themselves. If correct, this argument implies that net production of relief in these systems is probably limited to several hundred metres. It thus seems unlikely that significant amounts of isostatic peak uplift would be induced by a climate change that involves either enhanced fluvial erosivity or a transition to wet-based glacial erosion. □

Received 17 March; accepted 5 July 1999.

1. Koons, P. O. Modeling the topographic evolution of collisional belts. *Annu. Rev. Earth Planet. Sci.* **23**, 375–408 (1995).
2. Beaumont, C., Kamp, P., Hamilton, J. & Fullsack, P. The continental collision zone, South Island, New Zealand: Comparison of geodynamical models and observations. *J. Geophys. Res.* **101**, 3333–3359 (1996).
3. Gilchrist, A. R., Summerfield, M. A. & Cockburn, H. A. P. Landscape dissection, isostatic uplift, and the morphologic development of orogens. *Geology* **22**, 963–966 (1994).
4. Montgomery, D. R. Valley incision and the uplift of mountain peaks. *J. Geophys. Res.* **99**, 13913–13921 (1994).
5. Molnar, P. & England, P. Late Cenozoic uplift of mountain ranges and global climate change: Chicken or egg? *Nature* **346**, 29–34 (1990).
6. Small, E. E. & Anderson, R. S. Pleistocene relief production in Laramide mountain ranges, western United States. *Geology* **26**, 123–126 (1998).
7. Stuwe, K., White, L. & Brown, R. The influence of eroding topography on steady-state isotherms. Application to fission track analysis. *Earth Planet. Sci. Lett.* **124**, 63–74 (1994).
8. Mancktelow, N. S. & Grasemann, B. Time-dependent effects of heat advection and topography on cooling histories during erosion. *Tectonophysics* **270**, 167–195 (1997).
9. Raymo, M. E. & Ruddiman, W. F. Tectonic forcing of late Cenozoic climate. *Nature* **359**, 117–122 (1992).
10. Small, E. E. & Anderson, R. S. Geomorphically driven Late Cenozoic rock uplift in the Sierra Nevada, California. *Science* **270**, 277–280 (1995).
11. Brozovic, N., Burbank, D. & Meigs, A. Climatic limits on landscape development in the Northwestern Himalaya. *Science* **276**, 571–574 (1997).
12. Fielding, E. J., Isacks, B. L., Barazangi, M. & Duncan, C. How flat is Tibet? *Geology* **22**, 163–167 (1994).
13. Masek, J. G., Isacks, B. L., Gubbels, T. L. & Fielding, E. J. Erosion and tectonics at the margins of continental plateaus. *J. Geophys. Res.* **99**, 13941–13956 (1994).
14. Sklar, L. & Dietrich, W. E. in *Rivers Over Rock: Fluvial Processes in Bedrock Channels* (eds Tinkler, K. J. & Wohl, E. E.) 237–260 (AGU Press, Washington DC, 1998).
15. Montgomery, D. R. *et al.* Distribution of bedrock and alluvial channels in forested mountain drainage basins. *Nature* **381**, 587–589 (1996).
16. Montgomery, D. R. & Buffington, J. M. Channel-reach morphology in mountain drainage basins. *Geol. Soc. Am. Bull.* **109**, 596–611 (1997).
17. Montgomery, D. R. & Dietrich, W. E. Channel initiation and the problem of landscape scale. *Science* **255**, 826–830 (1992).
18. Schmidt, K. M. & Montgomery, D. R. Limits to relief. *Science* **270**, 617–620 (1995).
19. Burbank, D. W. *et al.* Bedrock incision, rock uplift and threshold hillslopes in the northwestern Himalayas. *Nature* **379**, 505–510 (1996).
20. Heimsath, A. M., Dietrich, W. E., Nishizumi, K. & Finkel, R. C. The soil production function and landscape equilibrium. *Nature* **388**, 358–361 (1997).
21. Hovius, N., Stark, C. P. & Allen, P. A. Sediment flux from a mountain belt derived by landslide mapping. *Geology* **25**, 231–234 (1997).
22. Hovius, N., Stark, C. P., Chu, H. T. & Lin, J. C. Supply and removal of sediment in a landslide-dominated mountain belt: Central Rang, Taiwan. *J. Geol.* (in the press).
23. Tucker, G. E. & Bras, R. L. Hillslope processes, drainage density, and landscape morphology. *Wat. Resour. Res.* **34**, 2751–2764 (1998).
24. Howard, A. D. in *Rivers Over Rock: Fluvial Processes in Bedrock Channels* (eds Tinkler, K. & Wohl, E. E.) 297–319 (AGU Press, Washington DC, 1998).
25. *Rivers Over Rock: Fluvial Processes in Bedrock Channels* (eds Tinkler, K. & Wohl, E. E.) 323 (AGU Press, Washington DC, 1998).
26. Whipple, K. X. & Tucker, G. E. Dynamics of bedrock channels in active orogens: Implications for height limits of mountain ranges, landscape response timescales, and research needs. *J. Geophys. Res.* **104**, 17661–17674 (1999).
27. Hack, J. T. Studies of longitudinal stream profiles in Virginia and Maryland. *US Geol. Surv. Prof. Pap.* **294-B**, 97 (1957).
28. Howard, A. D., Seidl, M. A. & Dietrich, W. E. Modeling fluvial erosion on regional to continental scales. *J. Geophys. Res.* **99**, 13971–13986 (1994).
29. Tarboton, D. G., Bras, R. L. & Rodriguez-Iturbe, I. Scaling and elevation in river networks. *Wat. Resour. Res.* **25**, 2037–2051 (1989).
30. Montgomery, D. R. & Foufoula-Georgiou, E. Channel network representation using digital elevation models. *Wat. Resour. Res.* **29**, 1178–1191 (1993).
31. Willgoose, G. A physical explanation for an observed area-slope-elevation relationship for catchments with declining relief. *Wat. Resour. Res.* **30**, 151–159 (1994).
32. Snyder, N. P., Whipple, K. X., Tucker, G. E. & Merritts, D. J. Landscape response to tectonic forcing: DEM analysis of stream profiles in the Mendocino triple junction region, northern California. *Geol. Soc. Am. Bull.* (in the press).
33. Hallet, B., Hunter, L. & Bogen, J. Rates of erosion and sediment evacuation by glaciers: a review of field data and their implications. *Glob. Planet. Change* **12**, 213–235 (1996).
34. Paterson, W. S. B. *The Physics of Glaciers* (Pergamon, New York, 1994).
35. Oerlemans, J. Numerical experiments on large-scale glacial erosion. *Z. Gletscherskunde Glazialgeol.* **20**, 107–126 (1984).
36. Harbor, J. M. Numerical modeling of the development of U-shaped valleys by glacial erosion. *Geol. Soc. Am. Bull.* **104**, 1364–1375 (1992).
37. Andrews, J. T. Glacier power, mass balances, velocities and erosion potential. *Z. Geomorphol. N. F. Suppl. Bd.* **13**, 1–17 (1972).
38. Small, E. E., Anderson, R. S., Repka, J. L. & Finkel, R. Erosion rates of alpine bedrock summit surfaces deduced from in situ <sup>10</sup>Be and <sup>26</sup>Al. *Earth Planet. Sci. Lett.* **150**, 413–425 (1997).

### Acknowledgements

This work was supported in part by the NSF (Continental Dynamics) and NASA (K.X.W.). We thank G. Tucker for discussions of relief evolution in active orogens, and D. Burbank, P. Molnar and E. Small for comments and suggestions.

Correspondence and requests for materials should be addressed to K.X.W. (e-mail: kxw@mit.edu).